Table 3
Clinical risk factors for disease-free survival ($n = 142$)

Parameters	Categories (number of patients)	Risk ratio	95% CI	P value
Age (years)	$\geq 65/< 65$ (68/74)	0.88	0.60–1.28	0.51
Gender	Male/female (106/36)	0.92	0.60–1.43	0.74
HBs Ag	Positive/negative (23/119)	0.76	0.44–1.32	0.33
HCV Ab	Positive/negative (100/42)	1.02	0.67–1.56	0.91
Child–Turcotte–Pugh score	B/A (33/109)	1.05	0.66–1.66	0.83
AFP (ng/ml)	$>20/\leq 20$ (94/48)	1.08	0.72–1.62	0.68
DCP (AU/ml)	$>62.5/\leq 62.5$ (66/76)	1.63	1.11–2.39	0.01
Degree of tumour differentiation	Moderately + poorly/well (117/25)	0.99	0.60–1.63	0.97
Tumour size (cm)	$T>2.0/T\leq 2.0$ (104/38)	1.87	1.17–3.00	0.008
Tumour number	Multifocal/solitary (64/78)	1.80	1.22–2.64	0.002
IM and/or VI	Positive/negative (57/85)	1.67	1.13–2.46	0.009
Fibrous capsular formation	Positive/negative (106/36)	1.05	0.67–1.63	0.82
Ki-67 LI (%)	$>20/\leq 20$ (70/72)	1.63	1.11–2.39	0.01
EBAG9 immunoreactivity	Positive/negative + borderline (83/59)	1.30	0.88–1.92	0.17

EBAG9; ER-binding fragment-associated antigen 9; HBs Ag, HBs Ag-positive; HCV Ab, HCV Ab-positive; AFP, alpha-fetoprotein; DCP, des-g-carboxy prothrombin; IM, intrahepatic metastasis; VI, vascular invasion; 95% CI, 95% Confidence Interval.

Another finding of the present study is that in the majority of HCC tissues that showed enhanced EBAG9/RCAS1 expression, expression was detected over the entire surface and cytoplasm of the cancer cells, rather than displaying the restricted distribution observed in non-cancerous tissues. This finding is consistent with observations on invasive ductal carcinoma cells of the breast, where it was found that normal mammary gland cells only expressed EBAG9/RCAS1 on their apical surface, whereas carcinoma cells showed enhanced expression without a polar distribution [3].

Of the various clinicopathological parameters, enhanced expression of EBAG9/RCAS1 was closely related to degree of tumour differentiation and increased Ki-67 LI. Ki-67 antigen is preferentially expressed during all active phases of the cell cycle (G_1, S, G_2 and M phases), but is absent in resting cells [28]. In addition, the Ki-67 LI has been reported to be well correlated with the uptake of bromodeoxyuridine (BrdU), a well accepted proliferation-associated marker [29,30]. Since Ki-67 staining does not require the *in vivo* injection of a specific agent, which is necessary in BrdU studies, Ki-67 is now widely used as a marker of cell proliferation including in human studies [31]. Therefore, our observation suggests that enhanced EBAG9/RCAS1 expression is associated with HCC tumour progression as represented by dedifferentiation and proliferation. Interestingly, tumours that showed a 'nodule-in-nodule' appearance displayed a variable degree of EBAG9/RCAS1 expression that depended on the degree of differentiation within the tumour, i.e. intense expression in the less differentiated regions and weak expression in the more highly differentiated regions (Fig. 2a). Similarly, lesions characterised by fibrous capsular infiltration had intense EBAG9/RCAS1 staining at the site of infiltration (Fig. 2b). These findings lend support to the link between the level of EBAG9/RCAS1 expression and tumour progression.

In contrast, EBAG9/RCAS1 was not associated with tumour metastasis (IM and/or VI) in our series, although a significant relationship between RCAS1 expression and VI was reported previously in Ref. [16]. All these results led us to conclude that EBAG9/RCAS1 is closely associated with tumour dedifferentiation and proliferation, but not in tumour metastasis, at least in resectable HCCs. In other words, EBAG9/RCAS1 presumably relates more to the growth of the primary tumour than to the development of tumour metastases. This view may be partially supported by an idea proposed recently on the basis of the results of cDNA microarray analysis, namely that different genes function at different stages of HCC evolution [32]. According to this view, HCC requires additional steps with further discrete genetic changes, i.e. dedifferentiation and proliferation, to gain the ability to metastasise. Our results may therefore imply that enhanced EBAG9/RCAS1 expression is an intermediate event in the multistep progression of HCC, unrelated to the final event characterised by the frequent occurrence of vascular invasion and resultant intrahepatic metastasis. In our series, there was no significant difference in disease-free survival between patients with positive and negative/borderline EBAG9 immunoreactivity. The results are consistent with the finding that enhanced EBAG9 expression was not associated with metastatic parameters such as IM and VI, which have been the strong factors predictive of poor prognosis in the previous studies [33,34]. Taken together, EBAG9 may not be a prognostic factor in patients with resectable HCC, however, we believe it is of value as a pathological marker of a specific stage of HCC tumour progression.

In conclusion, we observed weak, but discretely localised, expression of EBAG9/RCAS1 in non-cancerous normal and chronically diseased liver tissues, suggesting that EBAG9/RCAS1 is expressed in a positionally regulated fashion. We further found that the expression of this protein was enhanced in approximately half of the HCCs, and that this enhanced expression was characterised by loss of the localised staining pattern. Enhanced EBAG9/RCAS1 expression was correlated with tumour dedifferentiation and proliferation, but not with metastasis. Future investigation of the role of EBAG9/RCAS1 in non-cancerous and cancerous liver tissues should help to clarify the mechanism of HCC progression.

Acknowledgements

The authors wish to express their appreciation for the skillful technical assistance of Ms. Atsuko Takeuchi in immunohistochemistry. We also thank Ms. Akiko Hirose, Ms. Etsuko Tanaka, and Ms. Mihori Kato for other technical support. This work was supported by a grant-in-aid for scientific research (13671219) from the Ministry of Education, Science and Culture, Japan, and a grant from the Sato Memorial Foundation for Cancer Research.

References

1. Watanabe T, Inoue S, Hiroi H, Orimo A, Kawashima H, Muramatsu M. Isolation of estrogen-responsive genes with a CpG island library. *Mol Cell Biol* 1998, **18**, 442–449.
2. Tsuchiya F, Ikeda K, Tsutsumi O, *et al.* Molecular cloning and characterization of mouse EBAG9, homolog of a human cancer associated surface antigen: expression and regulation by estrogen. *Biochem Biophys Res Commun* 2001, **284**, 2–10.
3. Suzuki T, Inoue S, Kawabata W, *et al.* EBAG9/RCAS1 in human breast carcinoma: a possible factor in endocrine-immune interactions. *Br J Cancer* 2001, **85**, 1731–1737.
4. Sonoda K, Nakashima M, Kaku T, Kamura T, Nakano H, Watanabe T. A novel tumor-associated antigen expressed in human uterine and ovarian carcinomas. *Cancer* 1996, **77**, 1501–1509.
5. Nakashima M, Sonoda K, Watanabe T. Inhibition of cell growth and induction of apoptotic cell death by the human tumor-associated antigen RCAS1. *Nat Med* 1995, **5**, 938–942.
6. Sonoda K, Kaku T, Kamura T, Nakashima M, Watanabe T, Nakano H. Tumor-associated antigen 22-1-1 expression in the uterine cervical squamous neoplasias. *Clin Cancer Res* 1998, **4**, 1517–1520.
7. Iwasaki T, Nakashima M, Watanabe T, *et al.* Expression and prognostic significance in lung cancer of human tumor-associated antigen RCAS1. *Int J Cancer* 2002, **89**, 488–493.
8. Izumi M, Nakanishi Y, Yoshino I, Nakashima M, Watanabe T, Hara N. Expression of tumor-associated antigen RCAS1 correlates significantly with poor prognosis in nonsmall cell lung carcinoma. *Cancer* 2001, **82**, 446–451.
9. Takahashi H, Iizuka H, Nakashima M, *et al.* RCAS1 antigen is highly expressed in extramammary Paget's disease and in advanced stage squamous cell carcinoma of the skin. *J Dermatol Sci* 2001, **26**, 140–144.
10. Kubokawa M, Nakashima M, Yao T, *et al.* Aberrant intracellular localization of RCAS1 is associated with tumor progression of gastric cancer. *Int J Oncol* 2001, **19**, 695–700.
11. Oshikiri T, Hida Y, Miyamoto M, *et al.* RCAS1 as a tumour progression marker: an independent negative prognostic factor in gallbladder cancer. *Br J Cancer* 2001, **85**, 1922–1927.
12. Nakakubo Y, Hida Y, Miyamoto M, *et al.* The prognostic significance of RCAS1 expression in squamous cell carcinoma of the oesophagus. *Cancer Lett* 2002, **177**, 101–105.
13. Suzuoki M, Hida Y, Miyamoto M, *et al.* RCAS1 expression as a prognostic factor after curative surgery for extrahepatic bile duct carcinoma. *Ann Surg Oncol* 2002, **9**, 388–393.
14. Enjoji M, Nakashima M, Nishi H, *et al.* The tumor-associated antigen, RCAS1 can be expressed in immune-mediated diseases as well as in carcinomas of biliary tract. *J Hepatol* 2000, **36**, 786–792.
15. Hiraoka K, Hida Y, Miyamoto M, *et al.* High expression of tumor-associated antigen RCAS1 in pancreatic ductal adenocarcinoma is an unfavorable prognostic marker. *Int J Cancer* 2002, **99**, 418–423.
16. Noguchi K, Enjoji M, Nakamuta M, *et al.* Expression of a tumor-associated antigen RCAS1 in hepatocellular carcinoma. *Cancer Lett* 2001, **158**, 197–202.
17. Kojiro M, Nakashima O. Histopathologic evaluation of hepatocellular carcinoma with special reference to small early stage tumors. *Semin Liver Dis* 1999, **19**, 287–296.
18. Takayama T, Makuuchi M, Hirohashi S, *et al.* Early hepatocellular carcinoma as an entity with a high rate of surgical cure. *Hepatology* 1998, **28**, 1241–1246.
19. Liver Cancer Study Group of Japan. *The General Rules for the Clinical and Pathological Study of Primary Liver Cancer*, 4th edn. Tokyo, Kanehara & Co. Ltd, 2000 pp. 28–34.
20. Ng IOL, Na J, Lai ECS, Fan ST, Ng M. Ki-67 antigen expression in hepatocellular carcinoma using monoclonal antibody MIB1: a comparison with proliferating cell nuclear antigen. *Am J Clin Pathol* 1995, **104**, 313–318.
21. Ito Y, Matsuura N, Sakon M, *et al.* Both cell proliferation and apoptosis significantly predict shortened disease-free survival in hepatocellular carcinoma. *Br J Cancer* 1999, **81**, 747–751.
22. Nakamura S, Suzuki S, Sakaguchi T, *et al.* Surgical treatment of patients with mixed hepatocellular carcinoma and cholangiocarcinoma. *Cancer* 1996, **78**, 1671–1676.
23. Bradford MM. A rapid and sensitive method for the quantification of microgram quantities of protein utilizing the principle of protein-dye binding. *Anal Biochem* 1976, **72**, 248–254.
24. Pugh RNH, Murray-Lyon IM, Dawson JL, Pietroni MC, Williams R. Transection of the oesophagus for bleeding oesophageal varices. *Br J Surg* 1973, **60**, 646–649.
25. Kosuge T, Makuuchi M, Takayama T, Yamamoto J, Shimada K, Yamasaki S. Long-term results after resection of hepatocellular carcinoma: experience of 480 cases. *Hepato-gastroenterol* 1993, **40**, 328–332.
26. Cox D, Oakes D. *Analysis of Survival Data*. London, Chapman and Hall, 1983.
27. Sonoda K, Kaku T, Hirakawa T, *et al.* The clinical significance of tumor-associated antigen RCAS1 expression in the normal, hyperplastic, and malignant uterine endometrium. *Gynecol Oncol* 2000, **79**, 424–429.
28. Gerdes J, Lemke H, Baisch H, Wacker HH, Schwab U, Stein H. Cell cycle analysis of a cell proliferation-associated human nuclear antigen defined by the monoclonal antibody Ki-67. *J Immunol* 1984, **133**, 1710–1715.
29. Cher ML, Chew K, Rosenau W, Carroll PR. Cellular proliferation in prostatic adenocarcinoma as assessed by bromodeoxyuridine uptake and Ki-67 and PCNA expression. *Prostate* 1995, **26**, 87–93.

30. Goodson WH 3rd, Moore DH 2nd, Ljung BM, *et al.* The functional relationship between in vivo bromodeoxyuridine labeling index and Ki-67 proliferation index in human breast cancer. *Breast Cancer Res Treat* 1998, **49**, 155–164.
31. Scholzen T, Gerdes J. The Ki-67 protein: from the known and the unknown. *J Cell Physiol* 2000, **182**, 311–322.
32. Okabe H, Satoh S, Kato T, *et al.* Genome-wide analysis of gene expression in human hepatocellular carcinomas using cDNA microarray: identification of genes involved in viral carcinogenesis and tumor progression. *Cancer Res* 2001, **61**, 2129–2137.
33. The Liver Cancer Study Group of Japan. Predictive factors for long term prognosis after partial hepatectomy for patients with hepatocellular carcinoma in Japan. *Cancer* 1994, **74**, 2772–2780.
34. Yamamto J, Kosuge T, Takayama T, *et al.* Recurrence of hepatocellular carcinoma after surgery. *Br J Surg* 1996, **83**, 1219–1222.

Digestive Diseases and Sciences, Vol. 48, No. 3 (March 2003), pp. 570–580 (© 2003)

Idoxifene and Estradiol Enhance Antiapoptotic Activity Through Estrogen Receptor-β in Cultured Rat Hepatocytes

HIROSHI INOUE, MD,* ICHIRO SHIMIZU, MD,* GUANGMING LU, MD,* MINA ITONAGA,* XUEZHI CUI,* YOSHIHITO OKAMURA,† MASAYUKI SHONO, PhD,† HIROHITO HONDA, MD,* SATOSHI INOUE, MD,‡§ MASAMI MURAMATSU, MD,§ and SUSUMU ITO, MD*

Oxidative stress plays a causative role in the development of hepatic fibrosis and apoptosis. Estradiol (E2) is an antioxidant, and idoxifene is a tissue-specific selective estrogen-receptor modulator. We have previously demonstrated that E2 inhibits hepatic fibrosis in rat models of hepatic fibrosis and that the actions of E2 are mediated through estrogen receptors (ERs). This study reports on the antiapoptotic role of idoxifene and E2, and the functions of ER subtypes ER-α and ER-β in hepatocytes undergoing oxidative stress. Lipid peroxidation was induced in cultured rat hepatocytes with ferric nitrilotriacetate solution with idoxifene or E2. Oxidative stress-induced early apoptosis was linked to its ability to inhibit not only the expression of Bcl-2 and Bcl-X_L but the production of antioxidant enzymes as well and to stimulate Bad expression. Hepatocytes possessed functional ER-β, but not ER-α, to respond directly to idoxifene and E2. Idoxifene and E2 suppressed oxidative stress-induced reactive oxygen species generation and lipid peroxidation, and their antiapoptotic effects on the activation of activator protein-1 and nuclear factor-κB, the loss of antioxidant enzyme activity, and Bcl-2 family protein expression in early apoptotic hepatocytes were blocked by the pure ER antagonist ICI 182,780. Our results indicate that idoxifene and E2 could enhance antiapoptotic activity through ER-β during oxidative damage in hepatocytes.

KEY WORDS: idoxifene; estradiol; estrogen receptor-β; oxidative stress; apoptosis.

The direct response of cells to oxidative stress, including that caused by oxygen-derived free radicals, other reactive oxygen species (ROS), and lipid peroxidation, triggers multiple intracellular alterations (1), leading to apoptosis and necrosis. Apoptosis is an active, genetically programmed cell death process, which is characterized by a unique sequence of events, with morphological features that are distinct from necrosis.

Based on clinical information, chronic hepatitis C and B appear to be accompanied by higher levels of inflammation and to progress more rapidly in men than in women (2), and cirrhosis and hepatocellular carcinoma are predominantly a disease of men and postmenopausal women (3). It should be noted that estradiol (E2) is a potent endogenous antioxidant, which reduces lipid peroxide levels in liver and serum (4, 5). Oxidative stress serves as a link between hepatic injury and fibrosis (1, 6). Recently, our laboratory has showed that E2 suppressed hepatic fibrosis in rat models of hepatic fibrosis induced with pig serum and dimethylnitrosamine (7, 8), inhibited activation of the

Manuscript received January 26, 2002; revised manuscript received September 25, 2002; accepted December 2, 2002.

From the *Department of Digestive and Cardiovascular Medicine and †General Laboratory for Medical Research, Tokushima University School of Medicine, Kuramoto-cho, Tokushima 770-8503, Japan; and ‡Department of Biochemistry and §Research Center for Genomic Medicine, Saitama Medical School, Moroyama-machi, Iruma-gun, Saitama, 350-0495, Japan.

Address for reprint requests: Dr. Ichiro Shimizu, Department of Digestive and Cardiovascular Medicine, Tokushima University School of Medicine, Kuramoto-cho, Tokushima 770-8503, Japan.

0163-2116/03/0300-0570/0

nuclear factor (NF)-κB proinflammatory transcription factor in cultured rat hepatocytes undergoing oxidative stress (9), and attenuated iron-induced lipid peroxidation in rat liver mitochondria (9). Hepatic fibrosis is associated with inflammation and cell death, which accompanies repair processes and is a consequence of severe liver damage that occurs in many patients with chronic hepatitis C and B (1, 6). A preliminary report concluded that the concomitant administration of E2 with testosterone caused lower serum liver enzyme levels in a young male patient with chronic hepatitis C and irradiation-induced testicular dysfunction (10). These findings suggest that the putative antifibrogenic role of E2 in the liver may contribute to the sex-associated differences observed in the development of chronic viral hepatitis.

It is well known that the Bcl-2 protein suppresses apoptosis and is up-regulated by estrogen in several tissues (11–13), thus acting as a regulator of an antioxidant pathway (14). Bcl-2, Bcl-X_L, Bad, and Bax are members of the Bcl-2 family of proteins that play important roles in regulating cell survival and apoptosis. Many cells have unique enzymatic defense systems against oxidative stress, including the production of superoxide dismutase (SOD) and glutathione peroxidase (GPx), which play a critical role in protecting the cell from oxygen-derived free radicals and other ROS. In addition to Bcl-2, Bcl-X_L also prevents apoptosis in response to a wide variety of stimuli. Conversely, proapoptotic proteins, Bad and Bax, can accelerate death and in some instances are sufficient to cause apoptosis. The effects of E2 on SOD and GPx production and Bcl-2 family protein expression in the liver, however, are not absolutely clear at present.

It should be pointed out that the administration of estrogen *per se* in women poses some potential risks including breast cancer and endometrial abnormalities (15). Idoxifene is a tissue-specific selective estrogen receptor modulator (16), which acts in breast tissue as an estrogen antagonist through the same estrogen receptor (ER) -α as the natural steroid hormone (17). Idoxifene acts in bone as an estrogen agonist for osteoblasts through interaction with the osteoblast ER-α (18) and shows negligible agonist activity in human endometrial cells (18). The recent discovery of ER-β, a second ER isoform, seems to be an important additional factor in the mechanism of estrogen action and has an overlapping but nonidentical tissue distribution in comparison to ER-α. Within the same organ it often appears that the ER subtypes are expressed differentially, supporting the hypothesis that both receptors may have different biological functions (19, 20). Idoxifene was originally developed for the treatment of advanced breast cancer and the prevention of postmenopausal osteoporosis. Our recent report suggests that idoxifene functions as an antioxidant and protects hepatocytes from inflammatory cell injury by inhibiting NF-κB activation (9). However, little information is available relative to the antiapoptotic role of idoxifene as well as E2 and to the functions of ER subtypes in hepatocytes.

The present study was undertaken to explore the antiapoptotic role of idoxifene in cultured rat hepatocytes undergoing oxidative stress, in direct comparison to the natural hormone E2. In this study oxidative stress-induced early apoptosis was linked to its ability to inhibit not only the expression of Bcl-2 and Bcl-X_L but the production of SOD and GPx as well, and to stimulate Bad expression. Moreover, apoptotic stimuli to cultured cells induced the activation of activator protein-1 (AP-1) as well as NF-κB. Hepatocytes were observed to possess high levels of ER-β expression and low levels of ER-α expression. Idoxifene and E2 suppressed oxidative stress-induced ROS generation and lipid peroxidation, and their antioxidant and antiapoptotic effects on the activation of AP-1 and NF-κB, the production of SOD and GPx, and the Bcl-2 family protein expression in early apoptotic hepatocytes were blocked by the pure ER antagonist ICI 182,780 (21). These findings suggest that idoxifene and E2 could enhance antiapoptotic activity mainly through the ER-β in hepatocytes.

MATERIALS AND METHODS

Cell Culture. Hepatocytes were isolated from the livers of male (500–600 g) and female (300–400 g) Wistar rats by collagenase perfusion as described previously (22). Inocula of 5×10^5 cells were introduced into 35-mm-diam plastic dishes. The cells were cultured in 1 ml of Williams medium E (WE) supplemented with 5% fetal bovine serum (FBS), 100 units/ml penicillin, 100 μg/ml streptomycin, and 1% L-glutamine at 37°C in a 5% CO_2 atmosphere and 100% humidity. After 4 hr, the cell medium was removed, and lipid peroxidation was induced in the hepatocytes by incubation in serum-free WE with 100 μmol/liter of ferric nitrilotriacetate solution (FeNTA) (23) in the presence of idoxifene or βE2 (Wako, Osaka, Japan) with and without ICI 182,780 (Tocris Cookson, Ballwin, Missouri, USA) (20) at the indicated dose for 24 hr. Idoxifene, E2, and ICI 182,780 were initially prepared as an ethanolic stock solution (10^{-2} mol/liter) and then diluted in culture medium to the appropriate working solution concentration (e.g., 10 × the final concentration). The eventual damage of cultured hepatocytes in the presence of FeNTA was evaluated by measuring lactate dehydrogenase (LDH) activity in the culture medium as described elsewhere (9).

For the immunohistochemical examination of ER-α and ER-β, cells were fixed with 4% paraformaldehyde for 1 hr at 4°C, washed twice with ice-cold phosphate-buffered saline (PBS), and then incubated with 0.25% bovine testicular hyaluronidase for 30 min at 4°C. After the cells had been washed twice with PBS, they were incubated overnight at 4°C with a 1:100 dilution of a monoclonal antibody against human ER-α (1D5) (DAKO, Glostrup, Denmark) and a 1:200 dilution of a polyclonal antibody against human ER-β (H-150) (Santa Cruz Biotechnology, Santa Cruz, California, USA). After the samples were washed again, they

were incubated with a 1:200 dilution of biotin-conjugated rabbit anti-mouse IgG F(ab')2 or goat anti-rabbit IgG F(ab')2. Following incubation with the avidin–biotin complex (Vectastain R ABC reagent, Vector Laboratories, Burlingame, California, USA), the antigen-antibody complexes were visualized with diaminobenzidine and were photographed using a differential interference contrast (DIC) microscope (Axioskop, Carl Zeiss, Heidenheim, Germany). As a negative control, normal mouse IgG or normal rabbit IgG were substituted for the specific antibody at the same dilution. Paraffin sections of a normal rat ovary were used as a positive control.

Determination of Lipid Peroxidation. Lipid peroxidation in the cells was determined by measurement of the levels of malondialdehyde (MDA), an end product of lipid peroxidation, using a thiobarbiturate method, as described previously (23). For determining MDA, the cells were washed with PBS followed by harvesting with a rubber policeman and were used in the measurements.

Measurement of Intracellular ROS. Intracellular ROS was monitored by means of the 2',7'-dichlorofluorescein diacetate (H_2DCF-DA) assay, as previously reported (24). Hepatocytes treated with FeNTA were washed twice with Hanks' balanced salt solution. H_2DCF-DA dissolved in ethanol was added at a final concentration of 5 μM. After incubation for another 30 min at 37°C, the cells were washed twice and scraped in PBS. 2',7'-Dichlorofluorescein (DCF) fluorescence was measured using a spectrofluorometer (VersaFluor Fluorometer, BioRad, Hercules, California, USA) with excitation at 490 nm and emission at 520 nm. The sample from the control cells was used as a blank.

Western Blot Analysis. ER subtype proteins in cultured hepatocytes were detected immunologically using antibodies against ER-α (1:1000 dilution) and ER-β (1:1000 dilution). Bcl-2 family proteins, Bcl-2 (Transduction Laboratories, Lexington, Kentucky, USA; 1:500 dilution), Bcl-X_L (Transduction Laboratories; 1:500 dilution), Bad (Transduction Laboratories; 1:500 dilution), and Bax (Santa Cruz Biotechnology; 1:300 dilution), were also detected immunologically in the cells. Western blot analysis of I-κB-α (inhibitory subunit of NF-κB) was performed as described previously (9). Immunoreactive bands were visualized with an ECL western blotting detection system (chemiluminescence) kit (Amersham, Arlington Heights, Illinois, USA) as described elsewhere (7, 8), and evaluated by densitometric analysis. A rabbit antibody against β-actin (Biomedical Technologies, Stoughton, Massachusetts, USA) was used for the control of protein loading.

RT-PCR. For the analysis of ER-α and ER-β expression, cells were collected using Isogen (Nippon gene, Tokyo, Japan), and total RNA was prepared according to the manufacture's instructions. RT-PCR was performed using a one-step RNA PCR kit (AMV) (Takara, Kyoto, Japan). Briefly, 1 μg of total RNA for each sample was added to a PCR reaction. After reverse transcription (30 min at 50°C; 2 min at 94°C), 30 cycles of amplifications (1 min at 94°C; 1 min at 50°C; 1 min at 72°C) were performed. The PCR products were separated on a 2% agarose gel. The oligonucleotides, 5'-AGTCTCTGGAAGAGAAGGAC-3' and 5'-ATCTCCAGCAGCAGGTCAT- A-3' were used for amplification of the 229-bp fragment of rat ER-α mRNA (25). The oligonucleotides 5'-CATCAGTAACAAGGGCATGG-3' and 5'-CACTGAGACTGTAGGTTCTG-3' were used for amplification of the 192-bp fragment of rat ER-β mRNA (26). Rat ovary and yeast transfer RNA were used as positive and negative controls, respectively. To confirm their identity, the rat ER-α and ER-β PCR fragments were sequenced using a Sequenase version 2.0 kit (United States Biochemical, Cleveland, Ohio, USA).

Antioxidant Enzyme Assays. Cells were washed twice with ice-cold PBS and lysed directly in 150 μl of Tris buffer (50 mmol/liter Tris HCl, pH 7.5, 5 mmol/liter ethylenediaminetetraacetic acid, and 1 mmol/liter diethiothreitol). The cell-associated proteins were disrupted by sonication for 1 min. The suspension was then centrifuged at 14,000*g* for 30 min at 4°C. Aliquots of the supernatants were analyzed for antioxidant enzymes. Protein levels of a predominantly cytosolic copper, zinc-dependent SOD (CuZn-SOD) were detected using an enzyme-linked immunosorbent assay (ELISA) system kit (Amersham, Little Chalfont, UK). GPx activities were determined using a Cellular Glutathione Peroxidase Assay kit (Calbiochem, San Diego, California, USA). Enzyme assays were performed according to each manufacturer's recommended protocol. The results are expressed as nanograms of immunoreactive protein levels for CuZn-SOD and the units for GPx per milligram of protein. Protein concentrations were determined by the Lowry method, using bovine serum albumin as a standard.

Electrophoretic Mobility Shift Assay. Cellular extract proteins were prepared as described elsewhere (9). For electrophoretic mobility shift assay (EMSA), an oligonucleotide corresponding to the DNA binding consensus site for AP-1 or NF-κB was end-labeled with [γ^{-32}P]ATP and T4 polynucleotide kinase using an AP-1 family (T-cell activation) Gelshift kit or a NF-κB family (T-cell activation) Gelshift kit (Geneka Biotechnology, Quebec, Canada). Labeled double-stranded probe (1×10^5 cpm) was added to 5 μg of cellular extract protein, and EMSAs were carried out according to the manufacturer's recommended protocol. DNA protein complexes were resolved by electrophoresis on a 5% nondenaturing polyacrylamide gel in 1 × Tris glycine EDTA buffer. The bandshift was visualized by autoradiography. Competition was performed by addition of specific unlabeled double-stranded of oligonucleotide to the reaction mixture in 20- or 100-fold molar excess.

Early Apoptosis Detection by Flow Cytometry and Confocal Fluorescence Microscopy. A combination of FITC-conjugated annexin V and propidium iodide (PI) is a powerful and selective tool for measuring early apoptosis by flow cytometry and fluorescence microscopy. Cells were incubated with FeNTA in the presence of idoxifene or E2 for 24 hr, followed by the addition of annexin V-FITC and PI using an ANNEXIN V FITC kit (Immunotech, Marseille, France), according to the manufacturer's recommended protocol. Flow cytometric analysis was performed on an ELICS XL flow cytometer (Coulter, Hialeah, Florida, USA). To directly detect early apoptotic cells, fluorescence microscopic observation was made using laser scanning confocal microscopy (TCS-4D, Leica, Heidelberg, Germany).

Statistical Analysis. Data are presented as the means ± SD, unless otherwise indicated. Means were compared between two groups using Wilcoxon's signed-rank test and the Mann-Whitney U test. All P values are two-tailed. $P < 0.05$ was considered to be statistically significant.

RESULTS

Protein and Gene Expressions of ER-α and ER-β in Cultured Rat Hepatocytes in a State of Oxidative Stress. To confirm the specificity of the antibodies used

for ER-α (1D5) and ER-β (H-150), we first detected the signals for ER-α and ER-β in positive tissues, namely, the uterus and prostate, respectively. Staining for ER α was detected in the nuclei of glandular epithelium and stromal cells in the endometrium of the uterus, whereas ER β immunoreactivity was detected in nuclei of secretary epithelial cells of the prostate (data not shown). In the next step, we performed Western blot analysis of extracts from the rat ovaries, which are known to express both ER-α and ER-β. As shown in a previous study (20), 66- and 55-kDa bands were detected with the anti-ER-α and anti-ER-β antibodies, respectively. When lysates of freshly isolated hepatocytes (data not shown) and cultured hepatocytes (Figure 1A) obtained from male and female rats ($N = 5$ in each group) were analyzed by Western blotting in the same manner, we also found 66- and 55-kDa bands for ER-α and ER-β, respectively. The viability of freshly isolated hepatocytes was typically 90–95%, which was determined by trypan blue exclusion, and the contamination of the nonparenchymal cells (small cells) was less than 2%. A densitometric analysis revealed that the expression intensity of ER-β was significantly greater than that of ER-α, although ER subtype expression was not significantly different between freshly isolated and cultured hepatocytes (data not shown), cultures with and without FeNTA, or genders (Figure 1B). As shown in Figure 1C, a few hepatocytes had nuclear immunoreactivity for ER-α, whereas immunohistochemistry for ER-β showed a strong nuclear positivity in hepatocytes, but not in contaminating small cells, obtained from male (Figure 1C) and female (data not shown) animals. In addition, cytosolic ER-β was detected in hepatocytes. No significant deference in the cellular localization of ER-α and ER-β between treatment with and without FeNTA or genders was found (data not shown). In the negative control, the reaction of samples with normal IgG at the same dilution instead of the specific antibody showed no staining above background (data not shown).

The occurrence of ER-α and ER-β in cultured hepatocytes from both genders was also investigated by RT-PCR. Transcripts of 229 bp and 192 bp for ER-α and ER-β were detected in the rat ovary (positive control) (Figure 1D), but not in yeast transfer RNA (negative control) (data not shown). The messages for ER-α and ER-β were detected in RNA samples from hepatocytes from males (Figure 1D) and females (data not shown) with a 100% homology with the sequence for the rat ER subtype genes (25, 26).

Effects of Idoxifene and E2 on Antioxidant Enzyme Production, Expression of Bcl-2 Family Proteins, and Activation of AP-1 and NF-κB in Cultured Rat Hepatocytes in a State of Oxidative Stress. Increased levels of extracellular LDH (309 ± 61 units/ml), intracellular MDA (0.67 ± 0.11 μmol/liter), and ROS generation ($8.2 \pm 1.6 \times 10^3$/mg protein) were observed in hepatocytes, which had been incubated with FeNTA for 24 hr compared to controls (57 ± 12 units/ml, 0.16 ± 0.05 μmol/liter, $1.9 \pm 0.7 \times 10^3$/mg protein, respectively) (Figure 2A). However, the FeNTA enhancement of intracellular ROS generation and lipid peroxidation in the cultures was significantly inhibited by idoxifene in a dose-dependent manner (10^{-8}–10^{-6} mol/liter) and by E2 at a dose of 10^{-6} mol/liter (Figure 2A) (9). Moreover, assays of the levels of antioxidant enzymes in the cells revealed that oxidative stress significantly attenuated CuZn-SOD (3.3 ± 0.5 ng/mg protein) and GPx (0.70 ± 0.13 units/mg protein) levels, compared to controls (8.8 ± 1.7 ng/mg protein, 1.2 ± 0.29 units/mg protein, respectively). In addition, idoxifene, in the range of 10^{-8}–10^{-6} mol/liter and E2 at a dose of 10^{-6} mol/liter induced an increase in antioxidant enzyme levels, compared to the controls (Figure 2B). The effect of idoxifene was dose-dependent. The difference between the antioxidant effects of idoxifene and E2 at the same dose level (10^{-6} mol/liter) was not statistically significant (Figure 2).

To assess the functional integrity of endogenous ER-β presented thus far in hepatocytes, a separate series of competition experiments was conducted with the specific ER antagonist ICI 182,780 in the presence of idoxifene or E2. The inhibitory effects of idoxifene and E2 at 10^{-6} mol/liter on the loss of CuZn-SOD and GPx activity, the increased levels of LDH and MDA, and the induced ROS generation were blocked by ICI 182,780 in a dose-dependent manner (data not shown), which was complete at 10^{-6} mol/liter ICI 182,780 (Figure 2). Treatment with ICI 182,780 alone had no effect on antioxidant enzyme activity, levels of LDH and MDA, or ROS generation (data not shown).

The effects of idoxifene and E2 on the expression of Bcl-2 family proteins in cultured hepatocytes were examined using western blotting techniques. The present study revealed that oxidative stress decreased the expression of Bcl-2 and Bcl-X_L and increased Bad expression, although much controversy exists with respect to the expression of antiapoptotic Bcl-2 family members to liver injury (27–31). For the idoxifene- and E2-supplemented cultures, the Bcl-2 and Bcl-X_L proteins increased and the Bad protein decreased (Figure 3). The stimulation of Bcl-2 and Bcl-X_L expression and the Bad degradation by idoxifene was found to be dependent on idoxifene concentration. Treatment with ICI 182,780 led to a complete block of the idoxifene- and E2-mediated induction of Bcl-2 and Bcl-X_L and degradation of Bad (Figure 3). ICI 182,780 alone showed no effect on cell morphology or expression of the Bcl-2 families in hepatocytes incubated with or without FeNTA (data not shown). Bax expression was not affected by any treatment employed herein (Figure 3).

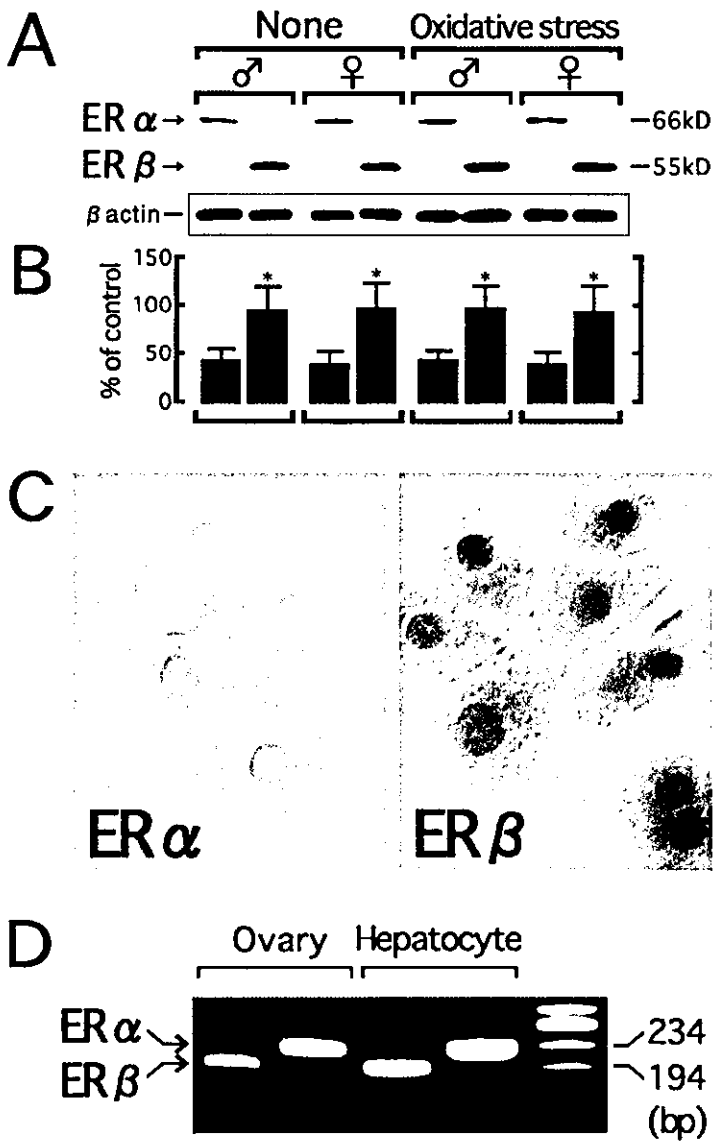

Fig 1. Western blot (A, B), immunohistochemical (C), and RT-PCR (D) analyses of ER-α and ER-β in cultured hepatocytes from male and female rats. (A) Cells were incubated with (Oxidative stress) and without (None) FeNTA in the presence of E2 (10^{-6} mol/liter) and Idoxifene (10^{-6} mol/liter) for 24 hr. Cell lysates were subjected to 12% sodium dodecyl sulfate–polyacrylamide gel electrophoresis and transferred onto nylon membranes, and ER subtypes were detected immunologically. The graphs represent typical results of five independent experments. (B) Densitometric analysis of ER subtype expression in hepatocytes shown in (A). The results of the densitometric analysis are expressed as mean persentages (± SD) of the values in β actin expression ($N = 5$ in each group). $^*P < 0.05$ compared to ER-α expression in FeNTA-nonsupplemented cultures. (C) Reaction of cultured hepatocytes from males with antibodies to ER-α and ER-β. Original magnification ×200. (D) RT-PCR showed 229- and 192-bp transcripts for ER-α and ER-β in cultured hepatocytes from males as well as ovaries as a positive control. One of four similar studies is shown.

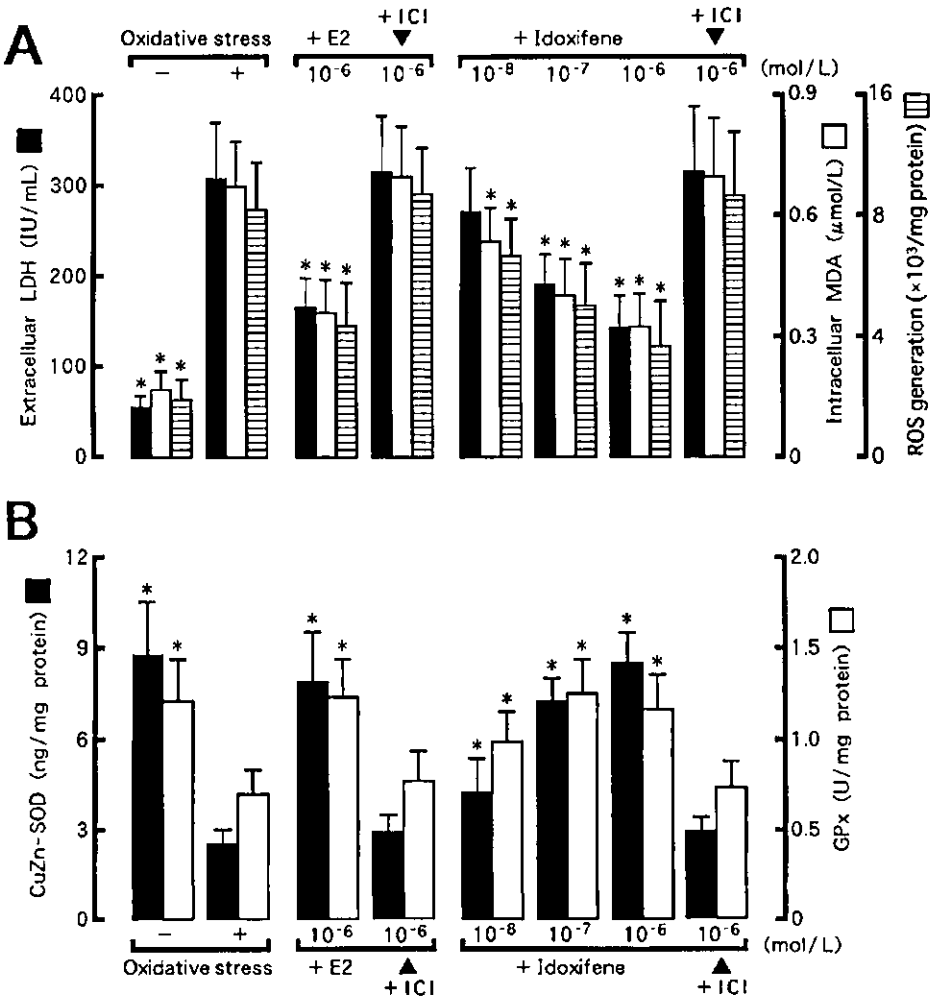

Fig 2. Effects of idoxifene and E2 on levels of extracellular LDH, intracellular MDA, and ROS generation (A) and levels of CuZn-SOD and GPx (B) in cultured hepatocytes in a state of oxidative stress. Cells were incubated with FeNTA (Oxidative stress) in the presence of E2 (10^{-6} mol/liter) and idoxifene (10^{-8}, 10^{-7}, and 10^{-6} mol/liter) with or without the ER antagonist ICI 182,780 (10^{-6} mol/liter) (ICI) for 24 hr. Values are means ± SD for 5 dishes. $^{*}P < 0.05$ compared to FeNTA-supplemented cultures.

AP-1 activation was determined by EMSA. The constitutive activity of AP-1 in hepatocyte cultures was quite low (Figure 4A). Following exposure to FeNTA, AP-1 was activated in a time-dependent manner. Activation of AP-1 as determined by EMSA was readily seen after 0.5 hr and reached maximal levels after 2 hr (Figure 4A). Idoxifene (10^{-6} mol/liter) caused a decrease in oxidative stress-induced AP-1 activation over a 24-hr period. The suppression of AP-1 activity was concentration-dependent within a concentration range of 10^{-8}–10^{-6} mol/liter idoxifene when assayed 2-hr after the induction of oxidative stress (Figure 4B). A similar dose-dependent suppression to that caused by idoxifene was observed in E2 (Figure 4B). The specificity of AP-1 DNA binding induced by oxidative stress was confirmed in competition experiments. Incubation with increasing doses of the cold unlabeled oligonucleotide led to the inhibition of binding activity (data not shown). Incubation with an excess of a mutant oligonucleotide did not antagonize AP-1 binding (data not shown). In addition, our preliminary report showed that oxidative stress induced the activation of NF-κB and the degradation of I-κB-α and treatment with idoxifene and E2 inhibited the I-κB-α degradation and NF-κB activation through the attenuation of hepatocyte oxidative bursts (9). The inhibitory effect of idoxifene and E2 on the activation of AP-1 (Figure 4B) and NF-κB and the I-κB-α degradation (Figure 4C, D) was blocked by ICI 182,780. Treatment with ICI 182,780 alone had no effect on the activation of AP-1 or NF-κB or the I-κB-α degradation (data not shown).

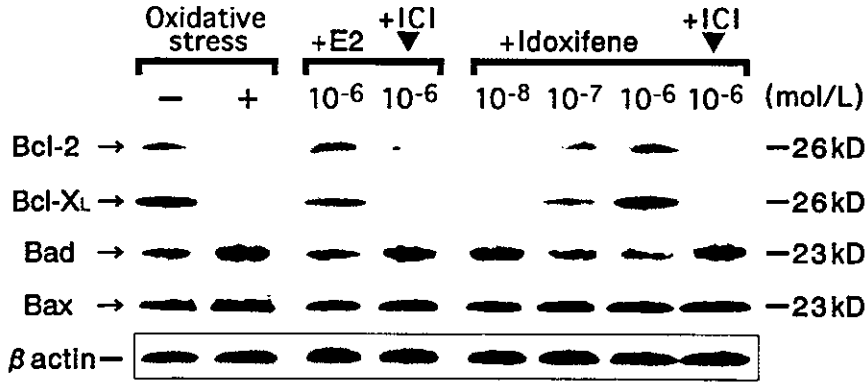

Fig 3. Effects of idoxifene and E2 on expression of Bcl-2 family proteins in cultured hepatocytes in a state of oxidative stress. Cells were incubated with FeNTA (Oxidative stress) in the presence of E2 (10^{-6} mlo/liter) and idoxifene (10^{-8}, 10^{-7}, and 10^{-6} mol/liter) with or without (10^{-6} mol/liter) ICI 182,780 (ICI) for 24 hr. Cell lysates were subjected to 12% sodium dodecyl sulfate–polyacrylamide gel electrophoresis and transferred onto nylon membranes, and Bcl-2 family proteins were detected immunologically. The graphs represent typical results of five independent experiments.

Apoptotic cells are stained by FITC-conjugated annexin V before the dying cell changes its morphology and its DNA undergoes hydrolysis (32). Early apoptotic cells contain high levels of FITC and low levels of PI signal, and in secondary necrotic cells both levels are high, while viable cells show low levels of both FITC and PI. A flow cytometric analysis of cultured hepatocytes with annexin V-FITC and PI demonstrated that the apoptotic cell population increased during 24 hr in culture, and was reduced at all time points when cells were cultured in the presence of idoxifene (10^{-6} mol/liter) (data not shown). Moreover, using laser scanning confocal microscopy, the FITC fluorescence, which was generated through apoptosis induced by oxidative stress, decreased in cells during idoxifene- and E2-supplemented culture (Figure 5A). The antiapoptotic activity of idoxifene was somewhat greater than that of the same dose of E2 (Figure 5B, C). ICI 182,780 treatment resulted in a complete block of the idoxifene- and E2-mediated induction of the antiapoptotic activity (Figure 5C).

DISCUSSION

In addition to ER action at a classical estrogen response element, ER-α and ER-β also mediate gene transcription from an AP-1 enhancer element. Paech et al reported that ER-α and ER-β from an AP-1 site signaled in opposite ways when combined with E2: with ER-α, E2 activated transcription, whereas with ER-β, E2 inhibited transcription (33). In the present study we demonstrate that high levels of ER-β and low levels of ER-α are expressed in hepatocytes in both oxidative stress and normal states from male and female rats and that the inhibitory effects of idoxifene and E2 on ROS generation and lipid peroxidation, LDH leakage, activation of AP-1 and NF-κB, and loss of antioxidant enzyme activity are blocked by ICI 182,780 in cultured rat hepatocytes undergoing oxidative stress. ICI 182,780 is one of a class of steroidal antiestrogens that bind ERs with an ER-β > ER-α binding affinity (34). Thus this compound acts as a pure antiestrogen on both receptor subtypes, especially ER-β. The present study also shows that ICI 182,780 blocked the hepatoprotective effect of idoxifene and E2 in a dose-dependent manner, which was complete at a dose of 10^{-6} mol/liter. We have also ruled out nonspecific toxic effects of the ER antagonist because it showed no effect on cell morphology, ER subtype expression, or the expressions of the Bcl-2 families in cultured hepatocytes incubated without FeNTA or estrogen agonists. These findings suggest that ER-β, not ER-α, mainly mediates the actions of idoxifene and E2 in hepatocytes.

Using immunohistochemistry, RT-PCR, and western blotting, Alvaro et al reported that no expression of ER-β was detected in male and female rat hepatocytes, whereas ER-α expression was detected in hepatocytes at a low level (35). Kuiper et al also detected the only mRNA expression of ER-α, but not ER-β, in rat livers by RT-PCR (36). These findings are contradictory to our result showing the presence of the ER-β gene by RT-PCR and ER-β protein by immunohistochemistry and western blotting in hepatocytes. In contrast, there are several reports that ER β protein and mRNA expression could be detected in rat livers and human fetus livers by immunohistochemistry, RT-PCR, and western and northern blotting (20, 37, 38). These discrepancy might be the result of the differences in the antibodies, primers, and immunohistochemical

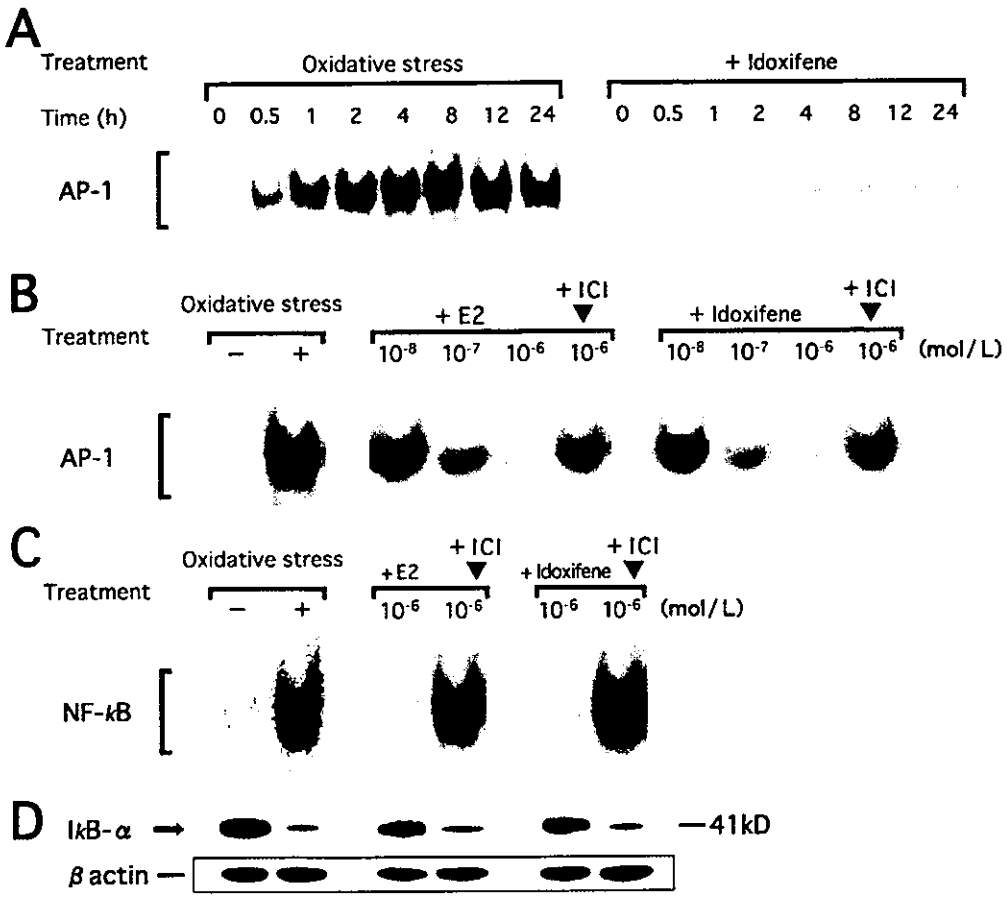

Fig 4. Effects of idoxifene and E2 on the activation of AP-1 and NF-κB in cultured hepatocytes in a state of oxidative stress. (A) Cells were incubated with FeNTA (Oxidative stress) in the presence of 10^{-6} mol/liter idoxifene for the indicated time (0–24 hr). Whole-cell extracts (5 μg) were assayed for AP-1 DNA binding activity by EMSA at the same time using the same labeled AP-1 probe. (B) Cells were incubated with FeNTA (Oxidative stress) in the presence of each substance at varying doses (10^{-8}, 10^{-7}, and 10^{-6} mol/liter) with or without 10^{-6} mol/liter ICI 182,780 (ICI) for 2 hr. The graphs represent typical results of four independent experiments. (C) Cells were incubated with FeNTA (Oxidative stress) in the presence of E2 (10^{-6} mol/liter) and idoxifene (10^{-6} mol/liter) with or without 10^{-6} mol/liter ICI 182,780 (ICI) for 2 hr. Whole-cell extracts (5 μg) were assayed for NF-κB DNA binding activity by EMSA using the same labeled NF-κB probe. (D) Effects of each substance (10^{-6} mol/liter) with or without 10^{-6} mol/liter ICI 182,780 (ICI), as shown in (C), on IκB-α expression. Equal amounts of whole-cell extracts were analyzed by western blotting using the I-κB-α antibody. The graphs represent typical results of five independent experiments.

procedures employed. Although nonparenchymal cells such as hepatic stellate cells (20) and cholangiocytes (35) are reported to express ER-β, and tissue culture conditions may lead to alterations of ER subtype expression (39, 40), the contamination of the nonparenchymal cells in the present study was less than 2%, and the expression levels of ER-β were higher in both freshly isolated and cultured hepatocytes than those of ER-α. In fact, immunohistochemistry for ER-β revealed a nuclear and cytosolic positivity in hepatocytes, but not in contaminating non-parenchymal cells. No significant differences in the intensity of ER β expression were detected between males and females. In contrast, a few hepatocytes had nuclear immunoreactivity for ER-α in both genders.

Furthermore, idoxifene and E2 were found to modulate Bcl-2 family protein expression in cultured hepatocytes exposed to FeNTA, in which oxidative stress-induced apoptosis was observed to be related to a decrease in Bcl-2 and Bcl-X_L expression and an increase in Bad expression, and act as an inhibitor early in the apoptotic pathway. The antiapoptotic intensity of idoxifene during oxidative stress-induced early apoptosis was similar to that of the same dose of E2. The specificity of the estrogen agonist-mediated antiapoptotic induction through the ER-β was shown by dose-dependent

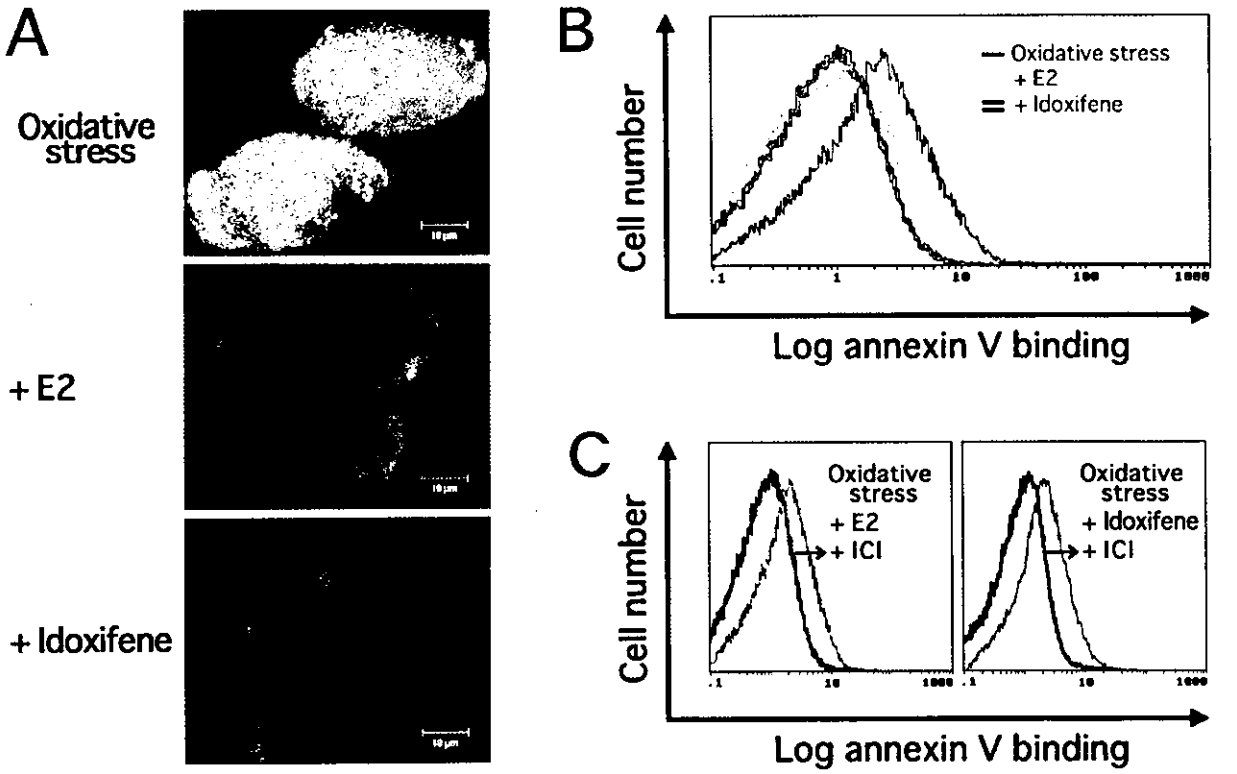

Fig 5. Effects of idoxifene and E2 on early apoptosis in hepatocytes using laser scanning confocal microscopy (A) and flow cytometry (B, C) with FITC-conjugated annexin V and PI. (A) Cells were incubated with FeNTA (Oxidative stress) in the presence of E2 (10^{-6} mol/liter) and idoxifene (10^{-6} mol/liter) for 24 hr, followed by the addition of annexin V-FITC and PI. Early apoptotic cells show both high FITC (green) and low PI (red) signals, secondary necrotic cells show both high signals, whereas viable cells show only low signals. (B) Cells were incubated with FeNTA (Oxidative stress) (thin lines) in the presence of E2 (10^{-6} mol/liter) (gray lines) and idoxifene (10^{-6} mol/liter) (thick lines) for 24 hr, followed by the addition of annexin V-FITC and PI. (C) Competitive effect of E2 or idoxifene (10^{-6} mol/liter) (thick lines) and the ER antagonist ICI 182,780 (10^{-6}mol/liter) (ICI) (thin lines) on early apoptosis induced with FeNTA (Oxidative stress). The graphs represent typical results of five independent experiments.

inhibition by ICI 182,780. However, several contradictory reports exists with respect to the expression of antiapoptotic Bcl-2 family members in animal livers with steatosis (29) and cholestasis (27). The conditions that favor cell damage (excessive damage and/or defective repair) would lead to apoptosis and/or necrosis, whereas these that favor of cell repair (reduced damage and/or enhanced repair) may lead to cell survival. Ray et al reported that mouse livers with apoptotic and necrotic cell death induced with acetaminophen, an inducer of oxidative stress, showed down-regulation of Bcl-X_L expression (30). In addition, *tert*-butylhydroperoxide was reported to induce oxidative stress and cell damage and to stimulate Bcl-2 disappearance from mitochondria in cultured rat hepatocytes (31). Bleomycin-induced apoptosis was also accompanied by decreases in Bcl-2 and Bcl-X_L protein levels in cultured mouse hepatocytes (28).

In previous studies, we showed that E2 inhibits iron-induced lipid peroxidation in rat liver mitochondria (9) and scavenges radicals (41). We also demonstrated that exogenous E2 functions as a fibrosuppressant via the inhibition of lipid peroxidation in rat models of hepatic fibrosis induced with pig serum and dimethylnitrosamine (7, 8). These effects of estrogen can be confirmed by blocking endogenous E2 with a specific antibody in male rats and by ovariectomy in female rats at the time of administration of dimethylnitrosamine (8). Moreover, studies with cultured rat hepatic stellate cells indicated that E2 suppresses the proliferation and fibrogenesis by these cells (7, 8). Hepatic stellate cells in the space of Disse undergo proliferation and transformation under inflammatory stimuli into myofibroblast-like cells and are responsible for much of the observed collagen hypersecretion and nodule formation that occurs during hepatic fibrosis to cirrhosis.

In contrast to E2, it has been reported that idoxifene differs from E2 in a tissue-specific manner. In reproductive tissues of the breast and uterus, where E2 is a potent agonist through the estrogen response element, idoxifene

shows activity for estrogen antagonism and/or minimal agonism (17, 18). In addition, idoxifene has estrogen agonism activity in the desired target tissue of bone (18). Although Treinen et al reported that idoxifene-related toxicity was evident at doses $\geq$0.03 mg/kg/day in rats and $\geq$0.1 mg/kg/day in rabbits, as evidenced by decreased body weight and/or food consumption (16), our preliminary data showed that treatment with idoxifene at doses of >0.1 mg/kg/day resulted in a significant inhibition in hepatic fibrosis in rats and caused no significant effects at the highest dose of 0.5 mg/kg/day on rat body weight, food consumption, and serum E2 levels (unpublished observations). The data presented here show the potential of idoxifene as an estrogen agonist in hepatocytes. Recently, Osborne et al reported that idoxifene derivatives are much less chemically reactive toward DNA than tamoxifen derivatives in both human and rat hepatocytes (42). Tamoxifen is similar to idoxifene in its chemical structure and is widely used in the treatment of estrogen receptor-positive breast cancer. However, tamoxifen has been shown to form DNA adducts and to induce liver cancer in rats (43). These findings indicate that idoxifene should be a safer drug for hepatoprotection.

Very recently we have reported that rat hepatic stellate cells express ER-β mRNA and protein, and that E2 is capable of inhibiting disruption of mitochondrial membrane potential in hepatic stellate cells undergoing early apoptosis (20). It has also been reported that E2 inhibits the proliferation of vascular smooth muscle cells (44, 45). Vascular smooth muscle cells are anatomically analogous to hepatic stellate cells and have been reported to express ER-β at a higher level after vascular injury without significant changes in ER-α expression (19). Artherosclerosis is predominantly a disease of men and postmenopausal women. Several studies document an antifibrotic effect of estrogen on vascular smooth muscle cells (46, 47). These findings and the preset data, which indicate that hepatocytes contain functional ER-β and that idoxifene and E2 can inhibit intracellular ROS generation and lipid peroxidation followed by antiapoptotic induction, suggest that these estrogen agonists may play a cytoprotective role through ER-β in these cells during chronic injury.

REFERENCES

1. Shimizu I: Antifibrogenic therapies in chronic HCV infection. Curr Drug Targets-Infectious Disorders 1:227–240, 2001
2. Poynard T, Bedossa P, Opolon P: Natural history of liver fibrosis progression in patients with chronic hepatitis C. Lancet 349:825–832, 1997
3. Shimizu I, Inoue H, Yano M, Shinomiya H, Wada S, Tsuji Y, Tsutsui A, Okamura S, Shibata H, Ito S: Estrogen receptor levels and lipid peroxidation in hepatocellular carcinoma with hepatitis C virus infection. Liver 21:342–349, 2001
4. Yoshino K, Komura S, Watanabe I, Nakagawa Y, Yagi K: Effect of estrogens on serum and liver lipid peroxide levels in mice. J Clin Biochem Nutr 3:233–239, 1987
5. Lacort M, Leal AM, Liza M, Martin C, Martinez R, Ruiz-Larrea MB: Protective effect of estrogens and catecholestrogens against peroxidative membrane damage *in vitro*. Lipids 30:141–146, 1995
6. Shimizu I: Sho-saiko-to: Japanese herbal medicine for protection against hepatic fibrosis and carcinoma. J Gastroenterol Hepatol 15:D84–D90, 2000
7. Shimizu I, Mizobuchi Y, Shiba M, Ma Y-R, Horie T, Liu F, Ito S: Inhibitory effect of estradiol on activation of rat hepatic stellate cells *in vivo* and *in vitro*. Gut 44:127–136, 1999
8. Yasuda M, Shimizu I, Shiba M, Ito S: Suppressive effects of estradiol on dimethylnitrosamine-induced fibrosis of the liver in rats. Hepatology 29:719–727, 1999
9. Omoya T, Shimizu I, Zhou Y, Okamura Y, Inoue H, Lu G, Itonaga M, Honda H, Nomura M, Ito S: Effects of idoxifene and estradiol on NF-κB activation in cultured rat hepatocytes undergoing oxidative stress. Liver 21:183–191, 2001
10. Shimizu I, Omoya T, Kondo Y, Kusaka Y, Tsutsui A, Shibata H, Honda H, Sano N, Ito S: Estrogen therapy in a male patient with chronic hepatitis C and irradiation-induced testicular dysfunction. Intern Med 40:100–104, 2001
11. Wang TT, Phang JM: Effects of estrogen on apoptotic pathways in human breast cancer cell line MCF-7. Cancer Res 55:2487–2489, 1995
12. Garcia-Segura LM, Cardona GP, Naftolin F, Chowen JA: Estradiol upregulates Bcl-2 expression in adult brain neurons. Neuroreport 9:593–597, 1998
13. Gohel A, McCarthy MB, Gronowicz G: Estrogen prevents glucocorticoid-induced apoptosis in osteoblasts *in vivo* and *in vitro*. Endocrinology 140:5339–5347, 1999
14. Hockenbery DM, Oltvai ZN, Yin XM, Milliman CL, Korsmeyer SJ: Bcl-2 functions in an antioxidant pathway to prevent apoptosis. Cell 75:241–251, 1993
15. Collaborative Group on Hormonal Factors in Breast Cancer: Breast cancer and hormone replacement therapy: collaborative reanalysis of data from 51 epidemiological studies of 52705 women with breast cancer and 108411 women without breast cancer. Lancet 351:1047–1059, 1997
16. Treinen KA, Rehm S, Wier PJ: An evaluation of the novel selective estrogen receptor modulator, idoxifene, for effects on reproduction in rats and rabbits. Toxicol Sci 41:199–207, 1998
17. Johnston SR, Boeddinghaus IM, Riddler S, Haynes BP, Hardcastle IR, Rowlands M, Grimshaw R, Jarman M, Dowsett M: Idoxifene antagonizes estradiol-dependent MCF-7 breast cancer xenograft growth through sustained induction of apoptosis. Cancer Res 59:3646–3651, 1999
18. Nuttall ME, Bradbeer JN, Stroup GB, Nadeau DP, Hoffman SJ, Zhao H, Rehm S, Gowen M: Idoxifene: a novel selective estrogen receptor modulator prevents bone loss and lowers cholesterol levels in ovariectomized rats and decreases uterine weight in intact rats. Endocrinology 139:5224–5234, 1998
19. Lindner V, Kim SK, Karas RH, Kuiper GG, Gustafsson JA, Mendelsohn ME: Increased expression of estrogen receptor-β mRNA in male blood vessels after vascular injury. Circ Res 83:224–229, 1998
20. Zhou Y, Shimizu I, Lu G, Itonaga M, Okamura Y, Shono M, Honda H, Inoue S, Muramatsu M, Ito S: Hepatic stellate cells contain the functional estrogen receptor β but not the estrogen receptor α in male

and female rats. Biochem Biophys Res Commun 286:1059–1065, 2001
21. Wakeling AE, Bowler J: ICI 182,780, a new antioestrogen with clinical potential. J Steroid Biochem Mol Biol 43:173–177, 1992
22. Shimizu I, Ichihara A, Nakamura T: Hepatocyte growth factor in ascites from patients with cirrhosis. J Biochem 109:14–18, 1991
23. Shimizu I, Ma Y-R, Mizobuchi Y, Liu F, Miura T, Nakai Y, Yasuda M, Shiba M, Horie T, Amagaya S, Kawada N, Hori H, Ito S: Effects of Sho-saiko-to, a Japanese herbal medicine, on hepatic fibrosis in rats. Hepatology 29:149–160, 1999
24. Maxwell DP, Wang Y, McIntosh L: The alternative oxidase lowers mitochondrial reactive oxygen production in plant cells. Proc Natl Acad Sci USA 96:8271–8276, 1999
25. Koike S, Sakai M, Muramatsu M: Molecular cloning and characterization of rat estrogen receptor cDNA. Nucleic Acids Res 15:2499–2513, 1987
26. Kuiper GG, Enmark E, Pelto-Huikko M, Nilsson S, Gustafsson JA: Cloning of a novel receptor expressed in rat prostate and ovary. Proc Natl Acad Sci USA 93:5925–5930, 1996
27. Kurosawa H, Que FG, Roberts LR, Fesmier PJ, Gores GJ: Hepatocytes in the bile duct-ligated rat express Bcl-2. Am J Physiol 272:G1587–G1593, 1997
28. Christensen JG, Gonzales AJ, Cattley RC, Goldsworthy TL: Regulation of apoptosis in mouse hepatocytes and alteration of apoptosis by nongenotoxic carcinogens. Cell Growth Differ 9:815–825, 1998
29. Rashid A, Wu TC, Huang CC, Chen CH, Lin HZ, Yang SQ, Lee FY, Diehl AM: Mitochondrial proteins that regulate apoptosis and necrosis are induced in mouse fatty liver. Hepatology 29:1131–1138, 1999
30. Ray SD, Balasubramanian G, Bagchi D, Reddy CS: Ca^{2+}-calmodulin antagonist chlorpromazine and poly(ADP-ribose) polymerase modulators 4-aminobenzamide and nicotinamide influence hepatic expression of BCL-XL and P53 and protect against acetaminophen- induced programmed and unprogrammed cell death in mice. Free Radic Biol Med 31:277–291, 2001
31. Haidara K, Morel I, Abalea V, Gascon BM, Denizeau F: Mechanism of *tert*-butylhydroperoxide induced apoptosis in rat hepatocytes: involvement of mitochondria and endoplasmic reticulum. Biochim Biophys Acta 1542:173–185, 2002
32. Martin SJ, Reutelingsperger CP, McGahon AJ, Rader JA, van Schie RC, LaFace DM, Green DR: Early redistribution of plasma membrane phosphatidylserine is a general feature of apoptosis regardless of the initiating stimulus: inhibition by overexpression of Bcl-2 and Abl. J Exp Med 182:1545–1556, 1995
33. Paech K, Webb P, Kuiper GG, Nilsson S, Gustafsson J, Kushner PJ, Scanlan TS: Differential ligand activation of estrogen receptors ERα and ERβ at AP1 sites. Science 277:1508–1510, 1997
34. Paige LA, Christensen DJ, Gron H, Norris JD, Gottlin EB, Padilla KM, Chang CY, Ballas LM, Hamilton PT, McDonnell DP, Fowlkes DM: Estrogen receptor (ER) modulators each induce distinct conformational changes in ER alpha and ER beta. Proc Natl Acad Sci USA 96:3999–4004, 1999
35. Alvaro D, Alpini G, Onori P, Perego L, Svegliata BG, Franchitto A, Baiocchi L, Glaser SS, Le Sage G, Folli F, Gaudio E: Estrogens stimulate proliferation of intrahepatic biliary epithelium in rats. Gastroenterology 119:1681–1691, 2000
36. Kuiper GG, Carlsson B, Grandien K, Enmark E, Haggblad J, Nilsson S, Gustafsson JA: Comparison of the ligand binding specificity and transcript tissue distribution of estrogen receptors alpha and beta. Endocrinology 138:863–870, 1997
37. Brandenberger AW, Tee MK, Lee JY, Chao V, Jaffe RB: Tissue distribution of estrogen receptors alpha (ER-alpha) and beta (ER-beta) mRNA in the midgestational human fetus. J Clin Endocrinol Metab 82:3509–3512, 1997
38. Maruyama K, Endoh H, Sasaki-Iwaoka H, Kanou H, Shimaya E, Hashimoto S, Kato S, Kawashima H: A novel isoform of rat estrogen receptor beta with 18 amino acid insertion in the ligand binding domain as a putative dominant negative regular of estrogen action. Biochem Biophys Res Commun 246:142–147, 1998
39. Dickson RB, Eisenfeld AJ: 17 Alpha-ethinyl estradiol is more potent than estradiol in receptor interactions with isolated hepatic parenchymal cells. Endocrinology 108:1511–1518, 1981
40. Crabb DW, Roepke J: Loss of growth hormone-dependent characteristics of rat hepatocytes in culture. In Vitro Cell Dev Biol 23:303–307, 1987
41. Omoya T, Shimizu I, Liu F, Honda H, Ito S: Estradiol enhances biological defense activities against oxidative stress and prevents hepatic fibrosis. Hepatology 30:490A, 1999
42. Osborne MR, Hewer A, Davis W, Strain AJ, Keogh A, Hardcastle IR, Phillips DH: Idoxifene derivatives are less reactive to DNA than tamoxifen derivatives, both chemically and in human and rat liver cells. Carcinogenesis 20:293–297, 1999
43. Hard GC, Iatropoulos MJ, Jordan K, Radi L, Kaltenberg OP, Imondi AR, Williams GM: Major difference in the hepatocarcinogenicity and DNA adduct forming ability between toremifene and tamoxifen in female Crl:CD(BR) rats. Cancer Res 53:4534–4541, 1993
44. Fischer-Dzoga K, Wissler RW, Vesselinovitch D: The effect of estradiol on the proliferation of rabbit aortic medial tissue culture cells induced by hyperlipemic serum. Exp Mol Pathol 39:355–363, 1983
45. Vargas R, Wroblewska B, Rego A, Hatch J, Ramwell PW: Oestradiol inhibits smooth muscle cell proliferation of pig coronary artery. Br J Pharmacol 109:612–617, 1993
46. Iafrati MD, Karas RH, Aronovitz M, Kim S, Sullivan-TR J, Lubahn DB, O'Donnell-TF J, Korach KS, Mendelsohn ME: Estrogen inhibits the vascular injury response in estrogen receptor alpha-deficient mice. Nat Med 3:545–548, 1997
47. Bayard F, Clamens S, Meggetto F, Blaes N, Delsol G, Faye JC: Estrogen synthesis, estrogen metabolism, and functional estrogen receptors in rat arterial smooth muscle cells in culture. Endocrinology 136:1523–1529, 1995

Efp as a new molecular target for breast cancer therapy

Kuniko Horie[a], Tomohiko Urano[b] and Satoshi Inoue[a,b]

Anti-Cancer Drugs 2003, 14:1–2

[a]Research Center for Genomic Medicine, Saitama Medical School, Hidaka-shi, Saitama, Japan and [b]Department of Geriatric Medicine, Graduate School of Medicine, University of Tokyo, Tokyo, Japan.

Correspondence to S. Inoue, Research Center for Genomic Medicine, Saitama Medical School, 1397-1 Yamane, Hidaka-shi, Saitama 350-1241, Japan.
Tel: +81 429 85 7206; fax: +81 429 85 7209;
e-mail: INOUE-GER@h.u-tokyo.ac.jp

Received 17 September 2002 **Accepted** 1 October 2002

Breast cancer is the most common type of cancer among women in Western countries. Breast cancer is commonly treated by various combinations of surgery, radiation therapy, chemotherapy and hormone therapy. Prognosis and selection of therapy may be influenced by the age and menopausal status of the patient, stage of the disease, histological and nuclear grade of the primary tumor, estrogen-receptor (ER) and progesterone-receptor (PR) status, HER2/*neu* status, and inherited mutations in genes such as *BRCA1* and *BRCA2*.

Among several types of treatment, hormone therapy is generally considered as adjuvant systemic therapy for a postoperative patient with localized breast cancer or as first-line treatment for a postmenopausal patient with newly diagnosed metastatic disease. Most often, a selective estrogen receptor modulator (SERM) tamoxifen has been clinically used for years. Another SERM raloxifene has been recently shown to be effective in reducing the risk of invasive breast cancer [1]. The benefit of SERMs is restricted only to women with ER/PR-positive breast tumors. Evaluation of hormone receptor status as well as histological study of the tumor specimen is clinically important for predicting response to hormone therapy. Patients with advanced stages of metastases who have received an antiestrogen within the past year are given a second-line hormone therapy. Selective aromatase inhibitors, such as anastrozole and letrozole, are used for those advanced patients, especially in the postmenopausal stage.

Antiestrogenic agents, however, are not basically effective in ER-negative tumors. Breast cancer that is initially responsive to an antiestrogenic agent sometimes acquires resistance against hormone therapy in advanced stage of the disease. Although tamoxifen is beneficial in ER/PR-positive tumors, there are, however, several critical side effects including development of endometrial cancer or an increased incidence of venous thrombosis and strokes. Venous thromboembolic events and vaginal bleeding events are lower in patients treated with aromatase inhibitors such as anastrozole [2]; however, osteoporosis due to estrogen deprivation is a significant side effect. Thus, new targeted therapy with minimal side effects must be developed for effective breast cancer treatment.

Why do tumors in advanced stages acquire resistance against hormone therapy? The molecular clue may lie in the mechanism of the estrogen actions in our bodies. We hypothesized that identification of new downstream molecules of the estrogen receptor signaling pathway may provide some answers. Using genomic-binding site cloning techniques, our group has identified several target genes of the estrogen receptor that include estrogen-responsive elements in their promotor-enhancer regions. Among the ER-downstream molecules, Efp, an estrogen-responsive RING finger protein of 630 amino acids, has the structure of the RING-finger B-box-coiled-coil (RBCC) motif including a RING finger, B-box-coiled-coil region and SPRY domain [3]. Interestingly, several other cancer-related RING finger proteins, including PML, as a responsible gene for acute pre-myelocytic leukemia when it fuses with RARα, and BRCA1, as a tumor suppressor gene for familial breast and ovarian cancers, have been identified. Efp is predominantly expressed in estrogen target tissues including mammary glands and uteri [4], and also in breast cancers [5]. Efp is essential for growth of female organs such as the uterus, since mice deficient in the Efp gene have an underdeveloped uterus [6].

The important question is whether Efp is a key molecule for breast tumor growth. The answer primarily came from experiments using nude mice inoculated with human breast cancer MCF7 cells [7]. When the tumor volume reached 300 mm^3, mice were treated with ovariectomy or with antisense or sense oligonucleotides. Efp antisense oligonucleotide efficiently reduced the size of tumor generated by MCF7 cells in those recipient mice. The growth of MCF7 cells was initially estrogen dependent; however, the cells overexpressing Efp could grow even in ovariectomized nude mice that have very low levels of circulating estrogen. These results implicate Efp as a critical determinant factor for progression of breast cancer of advanced stages, as increased expression levels of Efp could provide estrogen-independent tumor growth.

If Efp could function as an accelerator for breast tumor growth, what is the mechanism of Efp function in tumor cell proliferation? Recent advances of molecular research have revealed that some RING finger proteins bind to ubiquitin-conjugating enzymes and form complexes called ubiquitin ligases. Ubiquitin ligases bring specific degradation signals to protein substrates, i.e. a multi-ubiquitin chain linked to the substrates. Polyubiquitinated substrate proteins are then recognized and subsequently destroyed in the proteosome. This proteasome-dependent proteolytic system is important to eliminate misfolded or abnormal proteins as well as to confer short half-lives on specific normal proteins such as mitotic cyclins whose critical concentrations must change promptly with alterations in the state of a cell. To investigate whether Efp plays a role as a RING finger type of ubiquitin ligase and has a particular substrate, we performed yeast two-hybrid screening from a mouse embryo cDNA library using Efp as a bait. These screens led to the identification of 14-3-3σ as an Efp interacting clone [7]. 14-3-3σ is transcribed in a p53-dependent manner and has been shown to arrest the cell cycle, especially at the G_2/M phase, by sequestrating cdc2 in the cytoplasm [8]. Although 14-3-3σ is expressed in mammary glands, reduced levels of 14-3-3σ seem to be related to breast malignancy, as down-regulation of the protein [9] or hypermethylation of its promoter region [10] is reported in breast cancer. Experimental evidence suggests Efp may provide unlimited proliferation of breast cancer cells by accelerated destruction of 14-3-3σ that functions as one of the cell cycle brakes. In that mechanism, estrogen may be the initial factor that up-regulates Efp levels; however, once Efp levels are constitutively increased, estrogen may no longer be required to promote cell cycle progression by regulating Efp expression. This estrogen-independent overexpression of Efp causes down-regulation of 14-3-3σ, allowing tumor cells to continue proliferation. Thus, overexpression of Efp may be one of the reasons for advanced tumor resistance to hormone therapy.

It remains to be determined whether Efp plays a similar critical role in human breast tumor progression. Nonetheless, based on our findings in the mouse model system, we anticipate Efp could be used as a potential molecular target for clinical application that provides a promising future direction for breast cancer treatment. For example, if and when selective inhibitors for Efp are developed and utilized, such agents have the potential to reduce breast tumor growth with minimal side effects—a significant problem observed in current antiestrogenic therapies. Tumors resistant to previous antiestrogenic therapies could be regulated by anti-Efp agents if the tumors express Efp. Finally, another interesting issue is whether Efp could promote tumor growth in other endocrine-related cancers such as endometrial cancer. Future research efforts will elucidate a more precise mechanism of action of Efp in endocrine-related cancers and develop more powerful antiestrogenic agents that selectively inhibit Efp function.

References

1 Cummings SR, Eckert S, Krueger KA, Grady D, Powles TJ, Cauley JA, *et al.* The effect of raloxifene on risk of breast cancer in postmenopausal women: results from the MORE randomized trial. Multiple Outcomes of Raloxifene Evaluation. *J Am Med Ass* 1999; **281**:2189–2197.

2 Bonneterre J, Buzdar A, Nabholtz JM, Robertson JF, Thurlimann B, von Euler M, *et al.* Anastrozole is superior to tamoxifen as first-line therapy in hormone receptor positive advanced breast carcinoma. *Cancer* 2001; **92**:2247–2258.

3 Inoue S, Orimo A,, Hosoi T, Kondo S, Toyoshima H, Kondo T, *et al.* Genomic binding-site cloning reveals an estrogen-responsive gene that encodes a RING finger protein. *Proc Natl Acad Sci USA* 1993; **90**:11117–11121.

4 Orimo A, Inoue S, Ikeda K, Muramatsu M. Molecular cloning, structure, and expression of mouse estrogen-responsive finger protein Efp. Co-localization with estrogen receptor mRNA in target organs. *J Biol Chem* 1995; **270**:24406–24413.

5 Ikeda K, Orimo A, Higashi Y, Muramatsu M, Inoue S. Efp as a primary estrogen-responsive gene in human breast cancer. *FEBS Lett* 2000; **472**:9–13.

6 Orimo A, Inoue S, Minowa O, Tominaga N, Tomioka Y, Sato M, *et al.* Underdeveloped uterus and reduced estrogen responsiveness in mice with disruption of the estrogen-responsive finger protein gene, which is a direct target of estrogen receptor. *Proc Natl Acad Sci USA* 1999; **96**:12027–12032.

7 Urano T, Saito T, Tsukui T, Fujita M, Hosoi T, Muramatsu M, *et al.* Efp targets 14-3-3σ for proteolysis and promotes breast tumour growth. *Nature* 2002; **417**:871–875.

8 Chan TA, Hermeking H, Lengauer C, Kinzler KW, Vogelstein B. 14-3-3σ is required to prevent mitotic catastrophe after DNA damage. *Nature* 1999; **401**:616–620.

9 Vercoutter-Edouart AS, Lemoine J, Le Bourhis X, Louis H, Boilly B, Nurcombe V, *et al.* Proteomic analysis reveals that 14-3-3σ is down-regulated in human breast cancer cells. *Cancer Res* 2001; **61**:76–80.

10 Umbricht CB, Evron E, Gabrielson E, Ferguson A, Marks J, Sukumar S. Hypermethylation of 14-3-3σ (stratifin) is an early event in breast cancer. *Oncogene* 2001; **20**:3348–3353.

Expression of estrogen, progesterone and androgen receptors in the oviduct of developing, cycling and pre-implantation rats

A Okada[1,2], Y Ohta[2,3], S Inoue[3,4,5], H Hiroi[6], M Muramatsu[5] and T Iguchi[3,7]

[1]Safety Research Laboratories, Yamanouchi Pharmaceutical Co., Ltd, Itabashi, Tokyo 174–8511, Japan

[2]Laboratory of Animal Science, Department of Veterinary Science, Faculty of Agriculture, Tottori University, Tottori 680–8553, Japan

[3]CREST, Japan Science and Technology Corporation, Kawaguchi, Saitama 332–0012, Japan

[4]Department of Geriatric Medicine, Graduate School of Medicine, University of Tokyo, Tokyo 113–8655, Japan

[5]Research Center for Genomic Medicine, Saitama Medical School, Saitama 350–1241, Japan

[6]Department of Obstetrics and Gynecology, Graduate School of Medicine, University of Tokyo, Tokyo 113–8655, Japan

[7]Center for Integrative Bioscience, Okazaki National Research Institutes, and Department of Molecular Biomechanics, School of Life Science, Graduate University for Advanced Studies, Okazaki, Aichi 444–8585, Japan

(Requests for offprints should be addressed to T Iguchi; Email: taisen@nibb.ac.jp)

Abstract

To determine expression and localization of receptors for estrogen (ER), progesterone (PR) and androgen (AR), detailed immunohistochemical evaluations were performed in the Sprague–Dawley rat oviduct during pre- and neonatal development, estrous cycle and pre-implantation period. In addition, real-time RT-PCR studies were conducted to evaluate changes in ERα, ERβ, total PR (PR-A+B), PR-B and AR mRNA expressions. All receptors except for ERβ were detected in epithelial, and stromal or mesenchymal cells of the fetal and neonatal oviduct, and increased with development. During the estrous cycle and early pregnancy, ERα and PR-A+B were expressed in epithelial, stromal and muscle cells throughout the oviduct region, and showed changes in expression predominantly in the isthmus. Only a few epithelial cells in the infundibulum (INF) and ampulla (AMP) showed ERβ staining. AR was detected in stromal and muscle cells throughout the oviduct region, and in epithelial cells of the INF/AMP. Taken together, ERα, PR-A+B and AR were detected in the epithelium of the INF/AMP region, but all of these receptors were expressed in a distinct subset of epithelial cells which were negative for β-tubulin IV, a ciliated epithelial cell marker. These results contribute to a better understanding of the respective roles of ERs, PRs and AR in the rat oviduct.

Journal of Molecular Endocrinology (2003) **30,** 301–315

Introduction

The mammalian oviduct, or fallopian tube, is an organ known as the female reproductive tract that has a fundamental role in gamete transport, fertilization and subsequent early embryo development. Functions of the oviduct, as well as those of uterus and vagina, are believed to be regulated by two ovarian sex steroid hormones, estrogen and progesterone (P4) (Jansen 1984, Harper 1994). In most tissues, estrogen and P4 actions are mediated by estrogen receptor α (ERα) and estrogen receptor β (ERβ), and P4 receptor-A (PR-A) and P4 receptor-B (PR-B) respectively, belonging to the nuclear receptor superfamily of ligand-inducible transcription factors (Mangelsdorf *et al.* 1995). Evaluation of the expression and localization of these receptors is key in clarifying the mechanisms of estrogen and P4 actions on cell proliferation, cytodifferentiation and functional differentiation of the reproductive tissues. In the uterus and vagina, ERs and PRs expressions have been well documented. The use of ER or PR gene knockout (KO) mouse tissue has strongly suggested the importance of epithelial–stromal tissue/cell interaction in cell proliferation, cytodifferentiation and

Journal of Molecular Endocrinology (2003) **30,** 301–315 Online version via http://www.endocrinology.org
0952–5041/03/030–301 *Printed in Great Britain*

functional differentiation of uterine and vaginal cells (Cooke *et al.* 1997, 1998, Buchanan *et al.* 1998, Kurita *et al.* 2000*a*,*b*, 2001). However, few data regarding the expression and regulation of these receptors in the oviducts of mammals, except for humans and nonhuman primates, have been accumulated (Brenner & Slayden 1994). Neither has there been evaluation of the role of ERs and PRs using ER or PR KO mice. The reason for the lack of information about rodent oviductal ERs and PRs may be the difficulty of examination because of its smaller size and more complex morphological features compared with the uterus, which has no regional differences and only a single epithelial cell type. In contrast, the oviduct has a coiled structure and is composed of four different regions: the infundibulum (INF), ampulla (AMP), isthmus (IST) and uterotubal junction (UTJ). Depending on the oviductal region, there are at least two types of epithelial cells: ciliated epithelial cells and nonciliated or secretory epithelial cells. Therefore, cell- and region-specificity of ERα, ERβ, PR-A and PR-B expressions should be determined for better understanding of the molecular and cellular mechanisms of estrogen and P4 actions in the rat oviduct. Although some previous reports have revealed ERα and ERβ expressions in the rat oviduct (Saunders *et al.* 1997, Sar & Welsch 1999, Mowa & Iwanaga 2000*a*,*b*, Wang *et al.* 2000), details of cell- and region-dependency still have not been determined or are varied between the reports. Regarding oviductal PR expression, Li (1994) reported neonatal ontogeny in the mouse, but no reports of rat ontogeny and isoform expression, or in cycling and pre-implantation mice and rats were found.

Androgens have uterotrophic effects in intact and ovariectomized immature female rats (Armstrong *et al.* 1976), and testicular feminized female (T*fm*/T*fm*) mice showed impaired reproductive performance (Lyon & Glenister 1980), suggesting the importance of androgens in females as well as males. Androgens are known to exert their effects via androgen receptor (AR), which is another member of the nuclear receptor superfamily (Mangelsdorf *et al.* 1995), and AR mRNA expression has been reported in endometrium, endometrial glands and myometrium of the rat uterus (Hirai *et al.* 1994). However, the molecular mechanism of androgen action and the role of AR in the female reproductive tract have not yet been demonstrated. Weihua *et al.* (2002) have recently reported the essential role of AR in the estrogen-induced uterine epithelial cell proliferation of rats, and indicated that stromal AR amplified the ERα signal by induction of insulin-like growth factor-I, which is known to be produced in stromal cells and induces epithelial cell proliferation in a paracrine fashion. Moreover, direct inhibitory effects of the ERα/AR heterodimer on both ERα and AR transactivational properties have been reported (Panet-Raymond *et al.* 2000). Accordingly, identification of regional and cellular AR localization may allow a better understanding of not only the role of AR, but also the mechanism of estrogen action in the rat oviduct.

In this report, changes in mRNA expression and protein localization of ERα, ERβ, total PRs (PR-A+B), PR-B and AR were determined during the pre- and neonatal development, estrous cycle, and pre-implantation period in the rat oviduct using real-time RT-PCR and immunohistochemistry. In addition, to identify the epithelial cell types expressing steroid hormone receptors, β-tubulin IV was used as a ciliated epithelial cell marker (Renthal *et al.* 1993) in double immunohistochemical studies.

Materials and methods

Animals

Male and female Sprague–Dawley rats obtained from Charles River Japan, Inc. (Kanagawa, Japan) were used (13 weeks of age). Animals were housed individually in stainless-steel cages with controlled temperature (23 ± 2 °C) and relative humidity (55 ± 10%), and a 13 h light:11 h darkness cycle (0800–2100). Pellet food (CRF-1; Oriental Yeast Co., Ltd, Tokyo, Japan) and municipal tap water were freely available. The day on which sperm was found in the vaginal smear was designated as gestation day (GD) 0 or prenatal day (PD) 0, and the day when neonates were born was designated as neonatal day (ND) 0. The stage of the regular 4-day estrous cycle was specified by the vaginal smear examination using a light microscope every morning. For each total RNA and tissue preparation, ten oviducts were removed from five ether-anesthetized rats in each group (PD 15 and 19 from female fetuses, ND 0, 3, 5, 7, 10, 15 and 20 from female neonates, metestrus, diestrus,

proestrus and estrus from cycling rats, and GD 0, 1, 2, 3 and 4 from pregnant rats). All animals were maintained in accordance with the Institutional Guidelines for Care and Use of Laboratory Animals.

Total RNA preparation and real-time RT-PCR

Procedures for total RNA preparation and real-time RT-PCR were described previously (Okada *et al.* 2002*b*). Template total RNA (500 ng) treated with DNase I was reverse-transcribed by using SuperScript II RNase H$^-$ reverse transcriptase (Invitrogen Corp., Carlsbad, CA, USA) with oligo(dT)$_{12-18}$ primer for 50 min at 42 °C and then chilled on ice. An aliquot of generated cDNA was amplified with a pair of primers (ERα, forward 5′CTGACAATCGACGCCAGAA3′ and reverse 5′CAGCCTTCACAGGACCAGAC3′; ERβ, forward 5′CTTGCCCACTTGGAAACATC3′ and reverse 5′CCAAAGGTTGATTTTATGGCC3′; PR-A+B, forward 5′CTTTGTTTCCTCTGCAA AAATTG3′ and reverse 5′GTATACACGTAAG GCTTTCAGAAGG3′; PR-B, forward 5′CAGAC CAACCTGCAACCAGAA3′ and reverse 5′AGT CCTCACCAAAACCCTGGG3′; and AR, forward 5′ACCCTCCCATGGCACATTTT3′ and reverse 5′TTGGTTGGCACACAGCACAG3′) derived from rat mRNA sequences (GenBank Accession No. Y00102, U57439, L16922, M20133 and U06637 respectively). Primers for PR-A+B, and PR-B were designed to detect a sequence in the 3′-UTR common to the A and B isoforms, and in the 5′-UTR unique to the B isoform respectively. Glyceraldehyde-3-phosphate-dehydrogenase (GAPDH) was likewise amplified as an internal control (forward 5′TCTACCCACGGCAAGTT CAAT3′ and reverse 5′ACCCCATTTGATGTT AGCGG3′; GenBank M17701). Quantitative real-time PCR was carried out in an ABI Prism 7700 Sequence Detector (Applied Biosystems, Foster City, CA, USA) using SYBR Green PCR Master Mix reagent (Applied Biosystems) as the detector. PCR cycle parameters were 94 °C for 15 s, 60 °C for 30 s and 72 °C for 60 s, followed by a hold temperature for 10 min at 95 °C. The threshold parameter was set as the cycle at which each fluorescent signal was first detected above background, and the number of template copies present at the start of the reaction was determined at exponential increase by comparison with a standard scale prepared from rat genomic DNA (Clontech Laboratories, Inc., Palo Alto, CA, USA). The expression level of each target gene was calculated by standardizing the target gene copy number with the GAPDH copy number in a sample. Purity and specificity of all products were confirmed by omitting the reverse transcriptase, and by single melting temperature, appropriate size and their sequence. Analysis of results is based on duplicate samples from four independent experiments.

Antibodies

A mouse monoclonal antibody against ERα (6F11; Novocastra Laboratories Ltd, Newcastle upon Tyne, UK) was used at a dilution of 1:50. A rabbit polyclonal anti-rat ERβ antiserum against a synthesized peptide (CSSTEDSKNKESQNLQSQ) corresponding to the C-terminal amino acid residues 467–485 of rat ERβ protein was generated and affinity-purified as described previously (Hiroi *et al.* 1999, Okada *et al.* 2002*a*), and was used at a dilution of 1:100. A pre-diluted mouse monoclonal antibody against PR-A+B (10A9) was obtained from Immunotech (Marseille Cedex, France). The epitope of the PR antibody is located on the C-terminus of PR, which is a common domain between A and B isoforms. A rabbit polyclonal antiserum against AR (N-20; Santa Cruz Biotechnology, Inc., Santa Cruz, CA, USA) and a mouse monoclonal antibody against β-tubulin IV (ONS1A6; BioGenex, San Ramon, CA, USA) were used at a dilution of 1:200 and 1:250 respectively. Binding specificity of all antibodies has been previously established (Banerjee *et al.* 1992, Fisher *et al.* 1997, Hiroi *et al.* 1999, Okada *et al.* 2002*b*, Pelletier *et al.* 2000, Weihua *et al.* 2002).

Tissue preparation and immunohistochemistry

Oviducts were fixed with 4% paraformaldehyde in 0·1 M phosphate buffer overnight at 4 °C. Sections cut in paraffin at 4 μm were deparaffinized and rehydrated. Antigen retrieval was performed by autoclaving at 121 °C for 15 min in 10 mM citrate buffer (pH 6·0) for ERα, PR-A+B and AR, or at 121 °C for 10 min in 0·8 M urea for ERβ. Sections were then rinsed in distilled water and treated with 0·3% hydrogen peroxide in methanol for 30 min at room temperature (RT). After rinsing in 0·01%

Triton X-100 in PBS (PBT), sections were blocked in normal sheep serum (Dako Corp., Carpinteria, CA, USA) for 30 min at RT, and then incubated overnight at 4 °C with the anti-ERα antibody or the anti-AR antibody, for 48 h at 4 °C with the anti-ERβ antibody, or for 2 h at RT with the anti-PR-A+B antibody. Following treatment with each primary antibody, sections were rinsed in PBT and treated with Simple Stain Rat PO (Nichirei, Tokyo, Japan) for 30 min at RT. After a final PBT wash, sections were treated with 0·01% 3,3′-diaminobenzidine tetrahydrochloride (Dojindo Laboratories, Kumamoto, Japan) in 0·05 M Tris–HCl at pH 7·6 including 0·068% imidazole (Sigma, St Louis, MO, USA) and 0·02% hydrogen peroxide for 5 min at RT.

For double immunohistochemistry, sections stained for ERα, PR-A+B or AR as described above were rinsed in PBT and blocked in normal sheep serum, followed by incubation with the anti-β-tubulin IV antibody overnight at 4 °C. Sections were rinsed in PBT and treated with EnVision/AP (Dako) for 30 min at RT. After rinsing in PBT, they were treated with fuchsin (Dako) including levamisole (Dako) for 5 min at RT.

All sections, except those for ERβ staining, were lightly counter-stained with hematoxylin (Dako A/S, Glostrup, Denmark). Normal mouse IgG (Dako A/S) and normal rabbit immunoglobulin fraction (Dako A/S) were used as negative controls in place of primary antibodies for ERα, PR-A+B, β-tubulin IV, and ERβ and AR stainings respectively, showing no specific immunoreactivity.

Immunohistochemical evaluation and statistical analysis

Sections were examined and photographed using a light-microscope (BX60; Olympus Optical Co., Ltd, Tokyo, Japan) attached to a digital camera (DP50; Olympus). Staining intensity was graded as negative, slight, weak, moderate or marked for ERα, ERβ, PR-A+B and AR immunohistochemistries. At least seven specimens from each of five animals were examined for all investigations.

Student's *t*-test or Welch's *t*-test were performed in cases of equal variance or unequal variance respectively, after ANOVA between oviduct, and uterus or prostate for comparison of gene expressions between tissues (Fig. 1). Duncan's multiple comparison test was carried out for changes in mRNA expression of ERα, ERβ, PR-A+B, PR-B and AR in the real-time RT-PCR study (Fig. 2). Data are represented as means ± S.D. and considered significantly different at $P<0·05$.

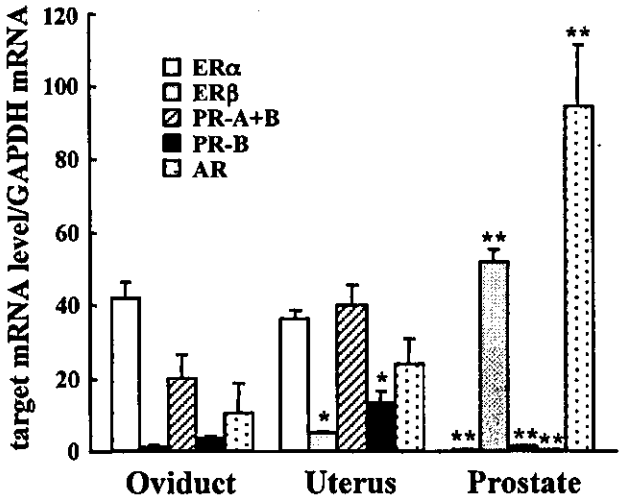

Figure 1 Comparison of ERα, ERβ, PR-A+B, PR-B and AR mRNA expressions by real-time RT-PCR between the oviduct, uterus and prostate. Data are represented as means±S.D. Analysis of results is based on duplicate samples each from three pooled total RNAs (three animals for each pooled sample). $^{**}P<0·01$ and $^{*}P<0·05$ vs oviduct.

Results

Expressions of ERα, ERβ, PR-A+B, PR-B and AR mRNAs in the rat oviduct

Quantitative real-time RT-PCR was employed to evaluate changes in expressions of ERs, PRs and AR mRNAs in the rat oviduct. First, to confirm the primers' specificity, expression levels for ERα, ERβ, PR-A+B, PR-B and AR mRNAs were determined in the diestrous uterus and prostate, as positive control tissues, in addition to the diestrous oviduct of the rats (Fig. 1). Expressions of ERα, PR-A+B and PR-B were much lower in the prostate than in the oviduct, while those of ERβ and AR were inversely highly in the prostate. The percentage for PR-B against PR-A+B was 33·8% in the uterus, being in agreement with previous reports (Ilenchuk & Walters 1987). Also, similar expression patterns for ERα, ERβ, PRs and AR in the rat prostate have been previously reported (Lau *et al.* 1998).